



Published in final edited form as:

Biochemistry. 2016 February 23; 55(7): 1159–1167. doi:10.1021/acs.biochem.5b01341.

FGF1 folding is critical for its nonclassical release

Igor Prudovsky^{1,3}, Doreen Kacer¹, Julie Davis², Varun Shah², Srinivas Jayanthi², Isabelle Huber², Rajalingam Dakshinamurthy², Owen Ganter⁴, Raffaella Soldi¹, David Neivandt³, Olgun Guvench^{4,3}, and Thallapuranam Krishnaswamy Suresh Kumar²

¹Maine Medical Center Research Institute, 81 Research Dr., Scarborough, ME 04074, (207) 396-8146

²Department of Chemistry and Biochemistry, University of Arkansas, Chemistry Bldg, University of Arkansas, Fayetteville, AR 72701, (479) 575-5646

³Graduate School of Biomedical Science and Engineering, University of Maine, Jenness Hall, University of Maine, Orono, ME 04469, (207) 581-2288

⁴College of Pharmacy, University of New England, Pharmacy Bldg, 716 Stevens Ave, Portland ME 04103, (207) 221-4171

Abstract

Fibroblast growth factor 1 (FGF1), a ubiquitously expressed proangiogenic protein that is involved in tissue repair, carcinogenesis and maintenance of vasculature stability, is released from the cells via a stress-dependent nonclassical secretory pathway. FGF1 secretion is the result of transmembrane translocation of this protein. It correlates with FGF1 ability to permeabilize membranes composed of acidic phospholipids. Similarly to several other nonclassically exported proteins, FGF1 exhibits β -barrel folding. To assess the role of FGF1 folding in its secretion, we applied targeted mutagenesis in combination with a complex of biophysical methods and molecular dynamics studies, followed by artificial membrane permeabilization and stress-induced release experiments. It has been demonstrated that a mutation of proline 135 located in the C-terminus of FGF1 results in: (i) partial unfolding of FGF1, (ii) decrease of FGF1 ability to permeabilize bilayers composed of phosphatidylserine, and (iii) drastic inhibition of stress-induced FGF1 export. Thus, FGF1 folding is critical for its nonclassical secretion.

Proteins released through the classical secretion pathway, which involves the endoplasmic reticulum (ER) and Golgi, usually have in their primary structure a cleavable hydrophobic signal peptide that determines their translocation to the lumen of the ER (1). However, a large group of secreted proteins are devoid of signal peptides, and their export does not depend on the ER-Golgi (2, 3). Among these nonclassically secreted proteins are potent regulators of cell differentiation, motility, proliferation, viability, and senescence (4, 5). Although the phenomenon of nonclassical protein secretion has been known for the last two decades, its exact mechanisms remain elusive. The export of several secreted signal peptide-

Correspondence to: Igor Prudovsky; Olgun Guvench; Thallapuranam Krishnaswamy Suresh Kumar.

Supporting Information Available:

Supplemental Figure 1 demonstrating that P135G mutation does not interfere with FGF1 binding to heparin

less proteins, such as HMGB1 (6), IL1 β (7, 8) and tissue transglutaminase (9) is mediated by non-ER-Golgi vesicular cytoplasmic organelles, which fuse with the cell membrane and release their contents to the extracellular compartment. In contrast, other nonclassically secreted proteins, including potent pro-angiogenic regulators fibroblast growth factor (FGF) 1 (10, 11) and FGF2 (12) exhibit diffuse distribution in the cytosol and are exported by direct translocation through the cell membrane.

Hyperthermia, hypoxia and other stress conditions exist in damaged and inflamed tissues and stimulate the export of FGF1 in tumors (13–15). We have shown that the stress-stimulated export of FGF1 is preceded by its translocation to the cell membrane (10). The export of FGF1 through the cell membrane correlates with the transmembrane translocation of the acidic phospholipid (PL), phosphatidylserine (PS) (11). Sum frequency generation vibrational spectroscopy (SFS) of immobilized PL membranes (16) and studies of induced fluorochrome release from liposomes (17, 18) demonstrated that FGF1 induces the disorganization of acidic PL membranes. Although several basic amino acids of the C-terminal domain FGF1 are important for its export (18), structural determinants underlying the export of FGF1 remain insufficiently studied. The experiments with FGF-DHFR chimeras inducibly locked in folded conformation demonstrated that unfolding is not required for the export of either FGF2 (19) or FGF1 (20). The passage of a protein across the membrane should require the contact with the hydrophobic membrane core. Interestingly, nonclassically released proteins FGF1, FGF2, and IL1 α are characterized by the β -barrel folding (4), which exposes hydrophobic residues and is found in many membrane proteins (21, 22). Most of the positively charged amino-acid residues of FGF1 are located in the C-terminal domain of this protein: in the β -sheets 10 and 11, and in the loops between β -sheets 10 and 11, and 11 and 12. We suggest that the β -barrel structure could be important for FGF1 export at the steps of membrane binding and/or transmembrane translocation. In this study, we applied a range of biophysical methods and the all-atom explicit-solvent molecular dynamics (MD) to further identify the importance of FGF1 folding for its export.

Materials and Methods

DNA constructs

Wild type (WT) α form of human FGF1 cDNA (23) was cloned into pET20b expression vector (24). FGF1 mutants were generated using Quick Change – II site-directed mutagenesis. All plasmids were subjected to DNA sequencing to verify their correctness. For expression in mammalian cells, WT and P135G mutant of FGF1 were cloned in pAdlox vector, as described (25).

Recombinant proteins

E. coli BL-21 pLysS cells were transformed with the respective plasmids. Cells were grown in LB broth and induced with 1mM IPTG for protein overexpression. Bacterial cells were harvested by centrifugation at 6000 rpm and subjected to cell lysis using ultra-sonication procedure with an output of 12 watts and an alternate on/off cycles for 10 seconds each in lysis buffer (10 mM sodium phosphate buffer; pH 7.2). Post-lysed cell suspension was centrifuged at 20000 rpm for 30 minutes to separate the clear cell lysate, which was loaded

onto the pre-equilibrated heparin sepharose column. Using a step gradient of sodium chloride concentration in the same buffer, WT and mutant proteins were eluted and further subjected to concentration and desalting using Millipore centrifugal ultra-concentrators. Concentration of the purified protein was estimated using spectrophotometry with A280 value.

Molecular dynamics simulation studies

Two solvated systems, one containing WT FGF1 and the other the P135G mutant, were constructed for all-atom explicit-solvent molecular dynamics simulations. FGF1 coordinates were from chain A in the 1.1 Å crystal structure of FGF1 (26). The N-terminal His tag was deleted and replaced with a single Met residue that corresponds to Met14 in the FGF1 sequence. Missing non-hydrogen atoms and the missing C-terminal residues Ser, Ser, Asp were constructed using force field geometries. The REDUCE algorithm (27) was used to add hydrogen atoms and to optimize the orientation of Asn and Gln sidechain amides and His sidechain imidazoles. Crystallographic water molecules within 5 Å of the protein were retained, and the protein was centered in a cube of bulk water molecules at experimental density and with edge length 20 Å longer than the FGF1 dimension along its longest principal axis. Bulk water molecules overlapping the protein were deleted, a random bulk water molecule was replaced with Cl⁻ to neutralize the system, and additional random water molecules were replaced with Na⁺ and Cl⁻ ions to yield 140 mM NaCl. Construction of the mutant followed the same protocol as for the WT FGF1 with the exception of computational introduction of the P135G mutation prior to solvation. Harmonic restraints were applied to FGF1 non-hydrogen atom positions, the system was energy minimized, and heated over 40 ps to 310 K. Harmonic restraints were then removed, and a 200 ns MD simulation at 310 K and 1 atm followed. Simulations employed periodic boundary conditions (28), Langevin thermostating with a friction coefficient of 0.1 ps⁻¹ (29), Langevin barostating (30), a 10 Å spherical cutoff, an energy-switching function applied to Lennard-Jones interactions between 8 to 10 Å (31), an isotropic correction to the pressure to account for Lennard-Jones interactions beyond the cutoff (28) and particle-mesh Ewald to account for electrostatic interactions beyond the cutoff (32). System construction and MD trajectory analysis utilized the CHARMM program (33), and MD simulation utilized the NAMD program (34). All simulations used the CHARMM biomolecular force field (35–38) and the TIP3P water model (39). Each of the two systems was simulated five times, with a different initial random seeds for each trajectory.

Differential Scanning Calorimetry

Recombinant protein samples of WT FGF1 and mutants at a concentration of 1mg/ml in 10 mM sodium phosphate buffer containing 100 mM NaCl, pH 7.2 was used to determine the melting temperature (T_m) on a Nano III DSC instrument (Delaware, USA). Prior to loading, all samples were subjected to degassing at 25°C for 15 minutes and after loading, the cells were equilibrated for 10 minutes at the same temperature. DSC was performed in the presence or absence of 0.5 mM sucrose octasulfate (SOS). To obtain a stable baseline, buffer blanks experiments were conducted before running the protein scans. Data obtained was processed using the software provided by the manufacturer to derive the thermodynamic parameters like T_m , H and S .

Limited Trypsin Digestion

Limited trypsin digestion of FGF1 WT and FGF1 mutants was performed in the absence or presence of SOS. With the addition of trypsin to protein at a ratio of 1 to 10 in 10 mM sodium phosphate buffer containing 100 mM NaCl; pH 7.2. An initial sample of undigested protein was removed prior to the addition of the enzyme, and the remaining trypsin-containing sample was incubated in a water bath at 37°C. Samples were removed every 5 minutes for the first 20 minutes, and then every 10 minutes until the 60-minute mark was reached. The reaction was stopped with the addition of 100% trichloroacetic acid. Samples were resolved on a 15% SDS-PAGE gel and subjected to Coomassie blue staining. Using UN-SacIT software (Silk Scientific Inc, Utah, USA), the bands corresponding to FGF1 were scanned and subjected to densitometry analysis to identify the percent digestion over time of incubation.

ANS Binding Studies

To determine the surface hydrophobicity of proteins, we used the sensitive and reliable 8-anilino-1-naphthalene sulfonic acid (ANS) binding assay, which requires very low concentrations of the protein sample. All spectra were collected on a Hitachi F-2500 spectrofluorometer with a slit width of 2.5 nm. Recombinant protein samples of WT FGF1 and mutants with a concentration of 50 μ M in 10 mM sodium phosphate buffer containing 100 mM NaCl, pH 7.2 were loaded into a quartz cuvette, ANS dye was added at increasing concentrations. ANS bound protein sample was excited at 380 nm at 25°C. Appropriate blank corrections were made to account for the effect of dilution. Spectra obtained were subjected to smoothing function provided by the manufacturer before collecting the values at 520 nm. Relative fluorescence intensity at 520 nm (emission maxima) was plotted against concentration of ANS.

NMR

Bacterial expression host *E. coli* BL-21 (DE3) cells were grown in M9 minimal medium containing $^{15}\text{NH}_4\text{Cl}$. To achieve maximal expression yield, medium was supplemented with necessary vitamins. Recombinant overexpressed proteins were subjected to uniform ^{15}N labeling. Multi-dimensional NMR experiments were carried out at 25°C on a Bruker Avance- μ 10 mM sodium phosphate buffer pH 7.2 with 10% D_2O added prior to acquisition of data. Spectra obtained were processed on Windows workstation using TopSpin v 2.5 and Sparky software.

Liposome permeabilization

Phosphatidylserine (PS) (AvantI) emulsion containing carboxyfluorescein dye was passed through the 1 μ m pore extruder to generate liposomes of uniform size as described (18). Unbound dye was separated from the dye containing liposomes using a size-exclusion chromatography on Superdex 75 (16/60 mm) column. WT, P25G or P135G FGF1 were added to liposomes to the concentration of 500 nM. Triton X100 (positive control of liposome permeabilization) was added to the concentration of 0.1%. Unquenching of fluorescence due to the release of dye from liposomes was quantified on Hitachi F-2500

spectrofluorometer. The excitation wavelength was at 492 nm with a slit width of 5 nm and emission was monitored at 517 nm with a slit width of 10 nm.

Cell culture

Murine NIH 3T3 cells (ATCC, Manassas, VA) were maintained in DMEM (HyClone, Logan, UT) supplemented with 10% bovine calf serum (HyClone).

Adenovirus production and transduction

Recombinant FGF1 WT and FGF1 P135G adenoviruses were produced, purified, and titered as described (25). Briefly, CRE8 cells were transfected with SfiI-digested pAdlox-derived constructs, and infected with the ψ 5 virus. The lysates were prepared 2 days after infection. The virus was passed twice through CRE8 cells, and purified from the second passage using a cesium density gradient. The virus was quantified by optical density at 260 nm, and the bioactivity was determined by a plaque-forming unit assay. Adenoviral transduction was performed in serum-free DMEM with approximately 10^3 viral particles/cell in the presence of poly-D-Lysine hydrobromide (Sigma) (5×10^3 molecules/viral particle) for 2 h at 37°C. Then the adenovirus-containing medium was removed and replaced with serum-containing medium. The cells were plated for experiments 24–48 h after transduction.

FGF1 export studies

NIH 3T3 cells were used to study FGF1 release 48 h after adenoviral transduction with FGF1 WT or P135G. The heat shock-induced FGF1 release assay was performed by incubation of the cells at 42°C for 110 min in serum-free DMEM containing 5 U/ml of heparin (Sigma), as previously described (13). Control cultures were incubated at 37°C for the same period. Conditioned media were collected, briefly centrifuged at 1,000 g to remove detached cells, and FGF1 was isolated for immunoblot analysis using heparin–Sepharose chromatography as described (13). Cell viability was assessed by measuring lactate dehydrogenase (LDH) activity in the medium using the Promega CytoTox kit (Promega, Madison, WI).

Results

Importance of Proline 135 located in the C-terminal portion of FGF1 for protein folding

Analysis of the 3D structure of FGF1 based on NMR results from the Kumar laboratory identified a number of amino acid residues as potential targets of mutagenesis intended to disrupt the β -barrel structure of these proteins (Figure 1). Particularly, it suggests that residue P135 located in the β -turn region of FGF-1 between the β -sheets 11 and 12 could be important for maintenance of the β -trefoil architecture of this protein. In the attempt to assess the role of FGF1 3D structure in its nonclassical secretion, we attempted to design a point mutation interfering with FGF1 folding. Single proline/glycine mutants in the positions 25, 41, 93, 135, 148 and 150 were produced and their folding characteristics were studied using biophysical methods. Differential scanning calorimetry demonstrated that all the studied mutations induced a moderate (3–6°C) decrease of the melting temperature of FGF1 (Table 1). We also used the limited proteolytic digestion to assess the conformational changes induced by proline mutations. Time-dependent trypsin digestion of FGF1 was

monitored by SDS-PAGE analysis. The degree of digestion was measured by densitometry on the basis of the intensity after Coomassie Blue staining of the 17kDa band on the polyacrylamide gel corresponding to undigested FGF1. Most studied mutations except P93G resulted in the increase of trypsin susceptibility of FGF1 (Figure 2A). Especially strong was the effect of P135G indicating that it induced a significant increase of the accessibility of normally hidden GHG1 domains to trypsin. In a parallel series of experiments, the effect of proline mutations on FGF1 folding was assessed by fluorometric determination of the binding of ANS, which is a hydrophobic fluorescent probe detecting the solvent-accessible non-polar surfaces in proteins (40). While most of proline mutations did not influence ANS binding, P135G mutation resulted in its significant increase (Figure 2B). Based on the results of trypsin digestion and ANS binding, we applied NMR to analyze the effect of P135G mutation on FGF1 structure. The overlay of the ^1H - ^{15}N HSQC spectra of WT and P135G FGF1 forms have shown the perturbation of many residues including those located more than 5 Å from the mutation site indicating that this mutation significantly disrupted protein folding (Figure 3).

Backbone conformation of wild-type and P135G FGF1 are similar

Molecular dynamics simulation time evolution of the root mean squared deviation of atomic positions relative to the starting crystallographic conformation (RMSD) shows FGF1 to be a flexible protein for its small size. WT RMSD values for the C α atoms reach as high as 8 Å, and this was also the case for P135G mutant (Figure 4A). Of note, sampling of conformations with large RMSD relative to the starting crystallographic conformation is often transient, with subsequent conformations from the same trajectory being closer to the crystal conformation. This suggests that the protein as simulated is not denaturing, but rather is highly flexible. This is confirmed by analysis of the root-mean-squared-fluctuation (RMSF) in C α positions. RMSF data for both WT and P135G FGF1 showed that, while the protein was flexible, this flexibility was limited to the N-terminal and C-terminal residues (Figure 4B). Starting at the N-terminal Met14, flexibility was very high (RMSF > 10 Å) but rapidly declined such that by residue 25, the RMSF value was less than 1 Å. Similarly, until the C-terminal residues was reached, RMSF values stayed low, consistent with a stable, folded protein. Only after residue 150 did RMSF values increase substantially, reaching values greater than 5 Å for the terminal residue Asp154. The final snapshots after 200-ns of MD sampling showed the consistency in the conformations for residues 25 to 150 as compared to the crystal structure (Figure 5A). In all cases, for both WT and P135G, the crystallographic barrel structure of this small protein was preserved.

From the RMSF data, there appears to be no significant effect of the P135G mutation on the ensemble of conformations that constitutes the folded state of FGF1. Notably, RMSF values for residues adjacent to and including the P135G mutation were unchanged relative to the WT protein (Figure 4B). Visual inspection of the P135G loop in the final snapshots largely confirmed this finding. All five of the WT trajectory final conformations had a loop structure like that of the starting crystal structure. This also held true for four of the five for P135G (Figure 5B). In the case of the fifth, there was loss of the short span of helical secondary structure. This lone example suggests a local destabilizing effect of the point mutation. Taken in the context of the NMR data, it appears that P135G does not change the

conformational properties of the folded state itself, but rather changes the thermodynamic balance between the folded state and the unfolded state, such that the folded state becomes relatively less stable.

Mutation of Proline 135 attenuates the permeabilization of phosphatidylserine membrane by FGF1 and inhibits its stress-induced export

We have previously shown that the mutations of Lysines 114,115, and 125,126 not only inhibit the stress-induced nonclassical export of FGF1, but also decrease the FGF1-induced destabilization of artificial membranes composed of acidic phospholipids (18). To assess the role of FGF1 folding in its ability to destabilize the membranes, we have chosen for the study of PS liposome permeabilization the P135G FGF1 mutant characterized by the strongest increase of protease sensitivity and ANS binding. We have used as controls WT FGF1 and the mutant P25G FGF1, which exhibited only a modest increase of protease sensitivity and ANS binding. While WT and P25G FGF1 caused a strong leakage of fluorochrome from PS liposomes, similar to that induced by Triton X100, the effect of P135G was significantly weaker (Figure 6A).

Next, the role of Proline 135 in FGF1 export was assessed. Preliminary studies demonstrated that P135G mutation did not interfere with FGF1 binding to heparin (Supplementary Figure 1), thus we used the standard heparin chromatography approach to assess the release of P135G FGF1 to the medium. NIH 3T3 cells were adenovirally transduced with WT or P135G FGF1 and subjected to 100 min incubation at 37°C or 42°C. Released FGF1 was isolated from the medium by adsorption to heparin-sepharose, resolved by SDS PAGE and detected by immunoblotting. We found that unlike WT FGF1, heat shock failed to induce the export of P135G FGF1 (Figure 6B)

Discussion

Understanding the structural determinants critical for nonclassical export of FGF1 is important for elucidating the mechanisms of its transmembrane translocation and developing approaches to regulation of the availability of this important biological regulator. Earlier studies (18, 41) demonstrated that the C-terminal portion of FGF1 enriched in basic amino acids is critical for its interaction with acidic PL present in the internal membrane leaflet. Here we report that the mutation of proline 135 localized in this domain disturbed the folding of FGF1 and blocked its stress-induced secretion. We have demonstrated that aminopterin-dependent stable folding of the dihydrofolate reductase (DHFR) moiety in FGF1-DHFR chimera does not prevent its stress-induced release (20). These data and earlier results of experiments with FGF2-DHFR (19) indicate that nonclassical FGF secretion does not require protein unfolding. The present study goes further by demonstrating the importance of FGF1 folding for its export. Although MD studies did not reveal significant conformation differences between folded WT and P135G FGF1, several biophysical and biochemical approaches including DSC, NMR, ANS binding and limited protease digestion clearly demonstrated a significant attenuation of FGF1 folding induced by P135G mutation. Rather than resulting in a permanent partial unfolding of FGF1, we suggest that this mutation changes the equilibrium between its folded and unfolded forms.

Nonclassical secretion of FGF1 and FGF2 involves their translocation through the plasma membrane and correlates with the ability of these proteins to destabilize bilayers containing acidic phospholipids (4, 42). Thus, mutations of basic amino acid residues in the C-terminal domain of FGF1 suppressed both its secretion and ability to destabilize artificial PS membranes (18). Similarly, as we have shown in the present study, a drastic inhibition of stress-induced FGF1 release by P135G mutation correlates with significantly attenuated permeabilization of the PS bilayer. The effect of P135G mutation on FGF1 secretion and membrane permeabilization may have different explanations. Thus, the specific folding of FGF1 could be critical for the exposure of C-terminal basic amino acids to the acidic phospholipids of the cell membrane and subsequent local membrane destabilization facilitating the translocation of this protein. On the other hand, the deterioration of the β -barrel structure by the P135 mutation may interfere with the formation of hydrophobic protein surface needed for FGF1 incorporation into the cell membrane. In this regard, it will be interesting to assess the effects of point mutations interfering with protein folding upon the nonclassical secretion of other β -barrel proteins such as FGF2 and IL1 α (4, 42). The finding about the importance of FGF1 folding for its secretion is promising for the development of cell permeable small molecules specifically binding FGF1 and inducing its partial unfolding, which would result in the inhibition of nonclassical protein secretion.

FGF1 is known to translocate across the membrane in a complex involving S100A13, a Ca²⁺ binding protein, and the p40 form of synaptotagmin 1 (Syt1), a cytosolic product of alternative translation of mRNA normally coding for transmembrane protein synaptotagmin 1 (4, 43, 44). FGF1 shares an interface with S100A13 and Syt1 interacts with phosphatidylserine, disrupting the lipid bilayer allowing translocation of the complex. By mapping the chemical shift perturbations of ¹H-¹⁵N HSQC, Mohan and coworkers revealed that the FGF1 binding site for S100A13 is composed of 14 residues: K98-F101 and R112-A122 (44). As a whole, FGF1 is characterized as a non-covalent complex during exportation (44). P135 is not reported to be involved in the interfacial region of the FGF1-S100A13 interaction, and therefore will have no direct effect on the stability of the formation of the FGF1-S100A13-p40Syt1 complex or complex attachment to the lipid bilayer. Furthermore, changing a hydrophobic proline to a hydrophobic glycine does not disrupt the charge character of the protein, thus effects on the stability of the secondary structure better evidence attenuation of membrane interaction as reported in this study.

Supplementary Material

Refer to Web version on PubMed Central for supplementary material.

Acknowledgments

Funding information: The study has been supported by Maine Medical Center institutional support to IP, a Maine Cancer Foundation grant to IP and NIH grant R01 HL35627 to IP. The work of TKSK group in this study was supported in part by grants from the NIH (NCRN COBRE Grant 1 P20 RR15569, P30 GM103450, R01 CA172631), the Department of Energy (Grant DE-FG02-01ER15161), National Science Foundation and the Arkansas Biosciences Institute.

In this work, we used the services of the Protein, Nucleic Acid and Cell Imaging Core and Recombinant Viral Vector Core supported by NIH grant P30 GM103392 to R. Friesel (Maine Medical Center Research Institute). This work also used the Extreme Science and Engineering Discovery Environment (XSEDE; allocation TG-

MCB120007) at the University of Arkansas, which is supported by the National Science Foundation (grant ACI-1053575). The authors have no conflict of interest to declare.

Abbreviations

ANS	8-anilino-naphthalenesulfonate
DSC	differential scanning calorimetry
FGF	fibroblast growth factor
HSQC	heteronuclear single quantum coherence
MD	molecular dynamics
NMR	nuclear magnetic resonance
PL	phospholipid
PS	phosphatidylserine
SOS	sucrose octasulfate
T_m	melting temperature
WT	wild-type

References

1. Blobel G. Protein targeting (Nobel lecture). *Chembiochem*. 2000; 1:86–102. [PubMed: 11828402]
2. Prudovsky I, Mandinova A, Soldi R, Bagala C, Graziani I, Landriscina M, Tarantini F, Duarte M, Bellum S, Doherty H, et al. The non-classical export routes: FGF1 and IL-1alpha point the way. *J Cell Sci*. 2003; 116:4871–4881. [PubMed: 14625381]
3. Nickel W, Seedorf M. Unconventional mechanisms of protein transport to the cell surface of eukaryotic cells. *Annu Rev Cell Dev Biol*. 2008; 24:287–308. [PubMed: 18590485]
4. Prudovsky I, Tarantini F, Landriscina M, Neivandt D, Soldi R, Kirov A, Small D, Kathir KM, Rajalingam D, Kumar TK. Secretion without Golgi. *J Cell Biochem*. 2008; 103:1327–1343. [PubMed: 17786931]
5. Prudovsky I. Nonclassically Secreted Regulators of Angiogenesis. *Angiol Open Access*. 2013; 1:1000101. [PubMed: 24511556]
6. Gardella S, Andrei C, Ferrera D, Lotti LV, Torrisi MR, Bianchi ME, Rubartelli A. The nuclear protein HMGB1 is secreted by monocytes via a non-classical, vesicle-mediated secretory pathway. *EMBO Rep*. 2002; 3:995–1001. [PubMed: 12231511]
7. Andrei C, Dazzi C, Lotti L, Torrisi MR, Chimini G, Rubartelli A. The secretory route of the leaderless protein interleukin 1beta involves exocytosis of endolysosome-related vesicles. *Mol Biol Cell*. 1999; 10:1463–1475. [PubMed: 10233156]
8. Dupont N, Jiang S, Pilli M, Ornatowski W, Bhattacharya D, Deretic V. Autophagy-based unconventional secretory pathway for extracellular delivery of IL-1beta. *EMBO J*. 2011; 30:4701–4711. [PubMed: 22068051]
9. Zemskov EA, Mikhailenko I, Hsia RC, Zaritskaya L, Belkin AM. Unconventional secretion of tissue transglutaminase involves phospholipid-dependent delivery into recycling endosomes. *PLoS One*. 2011; 6:e19414. [PubMed: 21556374]
10. Prudovsky I, Bagala C, Tarantini F, Mandinova A, Soldi R, Bellum S, Maciag T. The intracellular translocation of the components of the fibroblast growth factor 1 release complex precedes their assembly prior to export. *J Cell Biol*. 2002; 158:201–208. [PubMed: 12135982]

11. Kirov A, Al-Hashimi H, Solomon P, Mazur C, Thorpe PE, Sims PJ, Tarantini F, Kumar TK, Prudovsky I. Phosphatidylserine externalization and membrane blebbing are involved in the nonclassical export of FGF1. *J Cell Biochem.* 2012; 113:956–966. [PubMed: 22034063]
12. Schäfer T, Zentgraf H, Zehe C, Brügger B, Bernhagen J, Nickel W. Unconventional secretion of fibroblast growth factor 2 is mediated by direct translocation across the plasma membrane of mammalian cells. *J Biol Chem.* 2004; 279:6244–6251. [PubMed: 14645213]
13. Jackson A, Friedman S, Zhan X, Engleka KA, Forough R, Maciag T. Heat shock induces the release of fibroblast growth factor 1 from NIH 3T3 cells. *Proc Natl Acad Sci U S A.* 1992; 89:10691–10695. [PubMed: 1279690]
14. Mouta Carreira C, Landriscina M, Bellum S, Prudovsky I, Maciag T. The comparative release of FGF1 by hypoxia and temperature stress. *Growth Factors.* 2001; 18:277–285. [PubMed: 11519826]
15. Shin JT, Opalenik SR, Wehby JN, Mahesh VK, Jackson A, Tarantini F, Maciag T, Thompson JA. Serum-starvation induces the extracellular appearance of FGF-1. *Biochim Biophys Acta.* 1996; 1312:27–38. [PubMed: 8679713]
16. Doyle AW, Fick J, Himmelhaus M, Eck W, Graziani I, Prudovsky I, Grunze M, Maciag T, Neivandt D. Protein deformation of lipid hybrid bilayer membranes studied by Sum Frequency Generation Vibrational Spectroscopy (SFS). *Langmuir.* 2004; 20:8961–8965. [PubMed: 15461473]
17. Mach H, Middaugh CR. Interaction of partially structured states of acidic fibroblast growth factor with phospholipid membranes. *Biochemistry.* 1995; 34:9913–9920. [PubMed: 7543282]
18. Graziani I, Bagala C, Duarte M, Soldi R, Kolev V, Tarantini F, Kumar TK, Doyle A, Neivandt D, Yu C, et al. Release of FGF1 and p40 synaptotagmin 1 correlates with their membrane destabilizing ability. *Biochem Biophys Res Commun.* 2006
19. Backhaus R, Zehe C, Wegehingel S, Kehlenbach A, Schwappach B, Nickel W. Unconventional protein secretion: membrane translocation of FGF-2 does not require protein unfolding. *J Cell Sci.* 2004; 117:1727–1736. [PubMed: 15075234]
20. Graziani I, Doyle A, Sterling S, Kirov A, Tarantini F, Landriscina M, Kumar TK, Neivandt D, Prudovsky I. Protein folding does not prevent the nonclassical export of FGF1 and S100A13. *Biochem Biophys Res Commun.* 2009; 381:350–354. [PubMed: 19233122]
21. Wimley WC. The versatile beta-barrel membrane protein. *Curr Opin Struct Biol.* 2003; 13:404–411. [PubMed: 12948769]
22. Paschen SA, Waizenegger T, Stan T, Preuss M, Cyrklaff M, Hell K, Rapaport D, Neupert W. Evolutionary conservation of biogenesis of beta-barrel membrane proteins. *Nature.* 2003; 426:862–866. [PubMed: 14685243]
23. Forough R, Engleka K, Thompson JA, Jackson A, Imamura T, Maciag T. Differential expression in *Escherichia coli* of the alpha and beta forms of heparin-binding acidic fibroblast growth factor-1: potential role of RNA secondary structure. *Biochim Biophys Acta.* 1991; 1090:293–298. [PubMed: 1720023]
24. Rajalingam D, Graziani I, Prudovsky I, Yu C, Kumar TK. Relevance of partially structured states in the non-classical secretion of acidic fibroblast growth factor. *Biochemistry.* 2007; 46:9225–9238. [PubMed: 17636870]
25. Duarte M, Kolev V, Kacer D, Mouta-Bellum C, Soldi R, Graziani I, Kirov A, Friesel R, Liaw L, Small D, et al. Novel cross-talk between three cardiovascular regulators: thrombin cleavage fragment of Jagged1 induces fibroblast growth factor 1 expression and release. *Mol Biol Cell.* 2008; 19:4863–4874. [PubMed: 18784255]
26. Bernett MJ, Somasundaram T, Blaber M. An atomic resolution structure for human fibroblast growth factor 1. *Proteins.* 2004; 57:626–634. [PubMed: 15382229]
27. Word JM, Lovell SC, Richardson JS, Richardson DC. Asparagine and glutamine: using hydrogen atom contacts in the choice of side-chain amide orientation. *J Mol Biol.* 1999; 285:1735–1747. [PubMed: 9917408]
28. Allen, MP., Tildesley, DJ. *Computer Simulation of Liquids.* Oxford: Oxford University Press; 1987.
29. Kubo M, Czuwara-Ladykowska J, Moussa O, Markiewicz M, Smith E, Silver RM, Jablonska S, Blaszczyk M, Watson DK, Trojanowska M. Persistent down-regulation of Fli1, a suppressor of

- collagen transcription, in fibrotic scleroderma skin. *Am J Pathol.* 2003; 163:571–581. [PubMed: 12875977]
30. Feller SE, Zhang YH, Pastor RW, Brooks BR. Constant pressure molecular dynamics simulation: the Langevin piston method. *Journal of Chemical Physics.* 1995; 103:4613–4621.
 31. Steinbach PJ, Brooks BR. New spherical-cutoff methods for long-range forces in macromolecular simulation. *Journal of Computational Chemistry.* 1994; 15:667–683.
 32. Darden T, York D, Pedersen L. Particle mesh Ewald: an $N \cdot \log(N)$ method for Ewald sums in large systems. *Journal of Chemical Physics.* 1993; 98:10089–10092.
 33. Brooks BR, Brooks CL 3rd, Mackerell AD Jr, Nilsson L, Petrella RJ, Roux B, Won Y, Archontis G, Bartels C, Boresch S, et al. CHARMM: the biomolecular simulation program. *J Comput Chem.* 2009; 30:1545–1614. [PubMed: 19444816]
 34. Phillips JC, Braun R, Wang W, Gumbart J, Tajkhorshid E, Villa E, Chipot C, Skeel RD, Kale L, Schulten K. Scalable molecular dynamics with NAMD. *J Comput Chem.* 2005; 26:1781–1802. [PubMed: 16222654]
 35. Best RB, Zhu X, Shim J, Lopes PE, Mittal J, Feig M, Mackerell AD Jr. Optimization of the additive CHARMM all-atom protein force field targeting improved sampling of the backbone phi, psi and side-chain chi(1) and chi(2) dihedral angles. *Journal of Chemical Theory and Computation.* 2012; 8:3257–3273. [PubMed: 23341755]
 36. MacKerell AD Jr, Bashford D, Bellott M, Dunbrack RL, Evanseck JD, Field MJ, Fischer S, Gao J, Guo H, Ha S, et al. All-atom empirical potential for molecular modeling and dynamics studies of proteins. *Journal of Physical Chemistry B.* 1998; 102:3586–3616.
 37. MacKerell AD Jr, Feig M, Brooks CL III. Extending the treatment of backbone energetics in protein force fields: Limitations of gas-phase quantum mechanics in reproducing protein conformational distributions in molecular dynamics simulations. *Journal of Computational Chemistry.* 2004; 25:1400–1415. [PubMed: 15185334]
 38. Pastor RW, Mackerell AD Jr. Development of the CHARMM Force Field for Lipids. *J Phys Chem Lett.* 2011; 2:1526–1532. [PubMed: 21760975]
 39. Jorgensen WL, Chandrasekhar J, Madura JD, Impey RW, Klein ML. Comparison of simple potential functions for simulating liquid water. *Journal of Chemical Physics.* 1983; 79:926–935.
 40. Uversky VN, Winter S, Lober G. Use of fluorescence decay times of 8-ANS-protein complexes to study the conformational transitions in proteins which unfold through the molten globule state. *Biophys Chem.* 1996; 60:79–88. [PubMed: 8679928]
 41. Tarantini F, Gamble S, Jackson A, Maciag T. The cysteine residue responsible for the release of fibroblast growth factor-1 residues in a domain independent of the domain for phosphatidylserine binding. *J Biol Chem.* 1995; 270:29039–29042. [PubMed: 7493920]
 42. Nickel W, Rabouille C. Mechanisms of regulated unconventional protein secretion. *Nat Rev Mol Cell Biol.* 2009; 10:148–155. [PubMed: 19122676]
 43. Bagala C, Kolev V, Mandinova A, Soldi R, Mouta C, Graziani I, Prudovsky I, Maciag T. The alternative translation of synaptotagmin 1 mediates the non-classical release of FGF1. *Biochem Biophys Res Commun.* 2003; 310:1041–1047. [PubMed: 14559220]
 44. Mohan SK, Rani SG, Yu C. The heterohexameric complex structure, a component in the non-classical pathway for fibroblast growth factor 1 (FGF1) secretion. *J Biol Chem.* 2010; 285:15464–15475. [PubMed: 20220137]

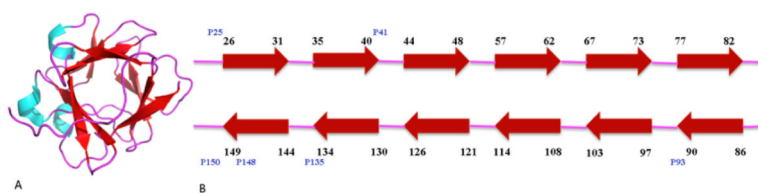
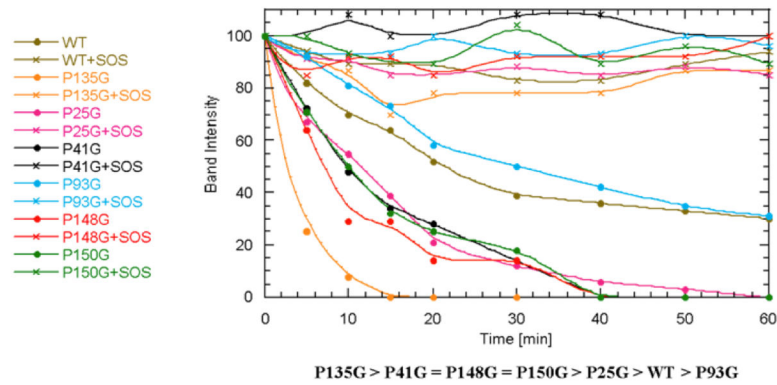


Figure 1. Three-dimensional β -barrel (A) and ribbon (B) structures of FGF1
 β -sheets are shown in red. Point mutations are discussed in the text. Downloaded from NCBI using the CN3D program.

A



B

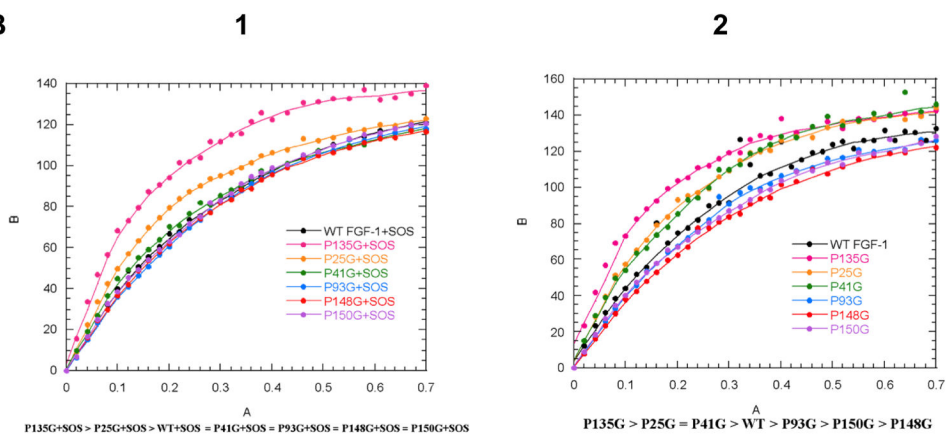


Figure 2. Effect of proline mutations on FGF1 folding

A. Trypsin sensitivity of proline/glycine mutants. B. ANS binding by proline/glycine mutants in presence (1) or absence (2) of SOS.

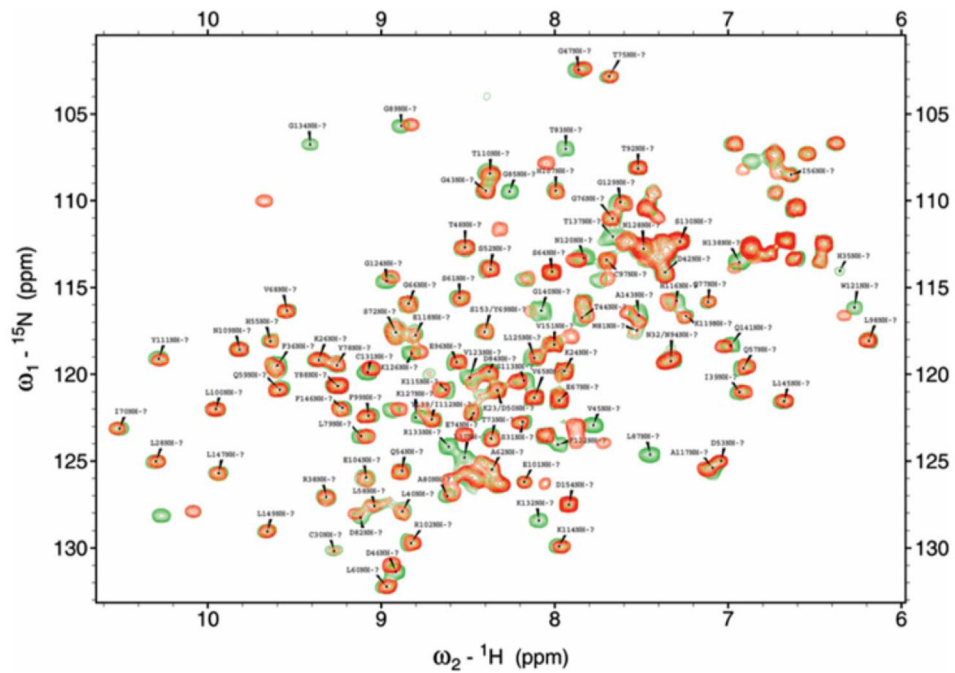


Figure 3. Overlay of the ^1H - ^{15}N HSQC spectra of the WT (red) and P135G (green) FGF1 forms. The distant residues located more than 5\AA from the mutation site are also perturbed indicating that the mutation disrupts the β -barrel architecture.

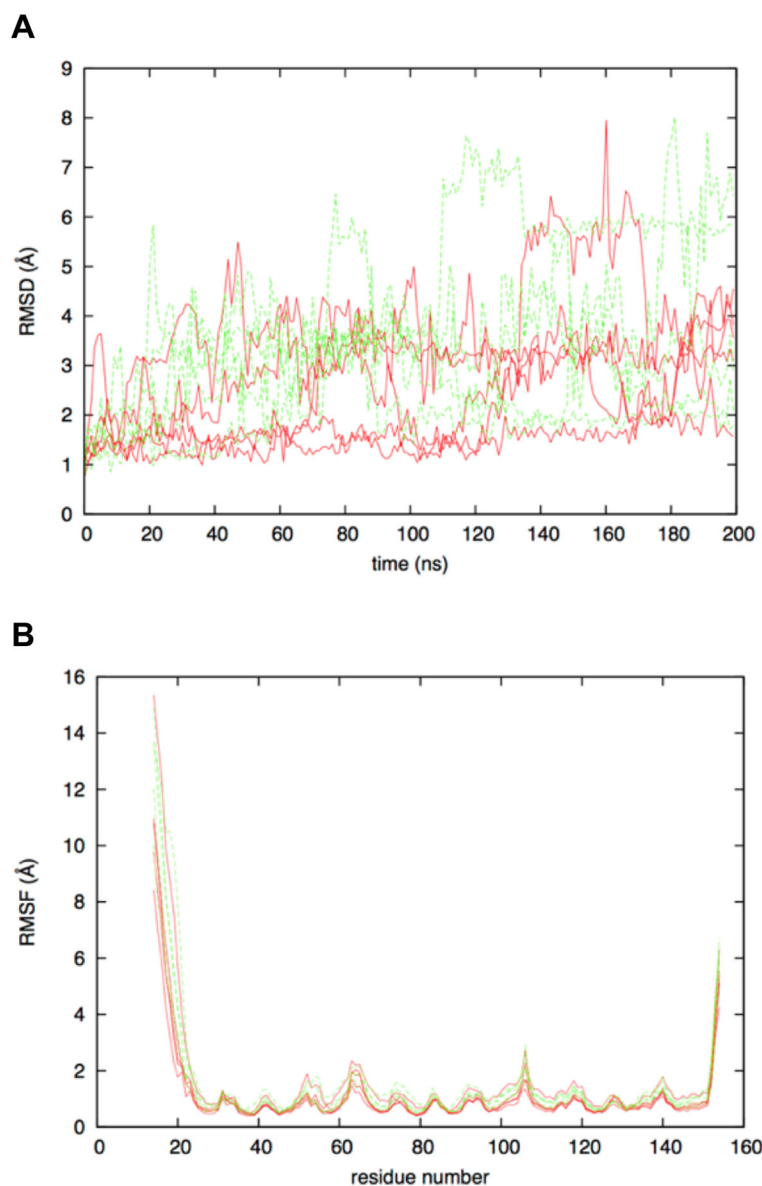


Figure 4. Flexibility in FGF1 as determined by molecular dynamics simulations
(A) Time evolution of C α atom RMSD. (B) C α atom root-mean-squared-fluctuation about time-averaged positions for the 20 ns to 200 ns interval. Data are shown for the five WT FGF1 (red) and five P135G FGF1 (green) trajectories. Values were computed after least-squares alignment of all C α atoms relative to the starting crystallographic conformation.

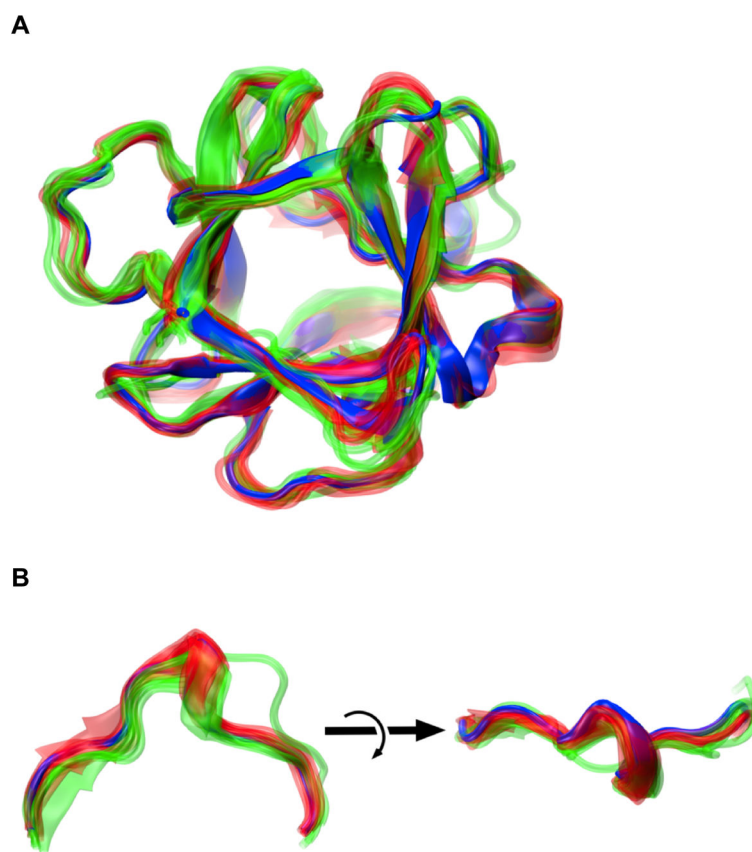


Figure 5. Structural consistency of residues 25 to 150 after MD simulation

(A) Ribbon representation for residues 25 to 150 are shown for the starting crystal conformation (solid blue), the five 200-ns time point MD snapshots for WT FGF1 (transparent red) and P135G FGF1 (transparent green). (B) Close-up of residues 130 to 140. MD snapshots were least-squares aligned to the crystallographic conformation using Ca atoms 25 to 150.

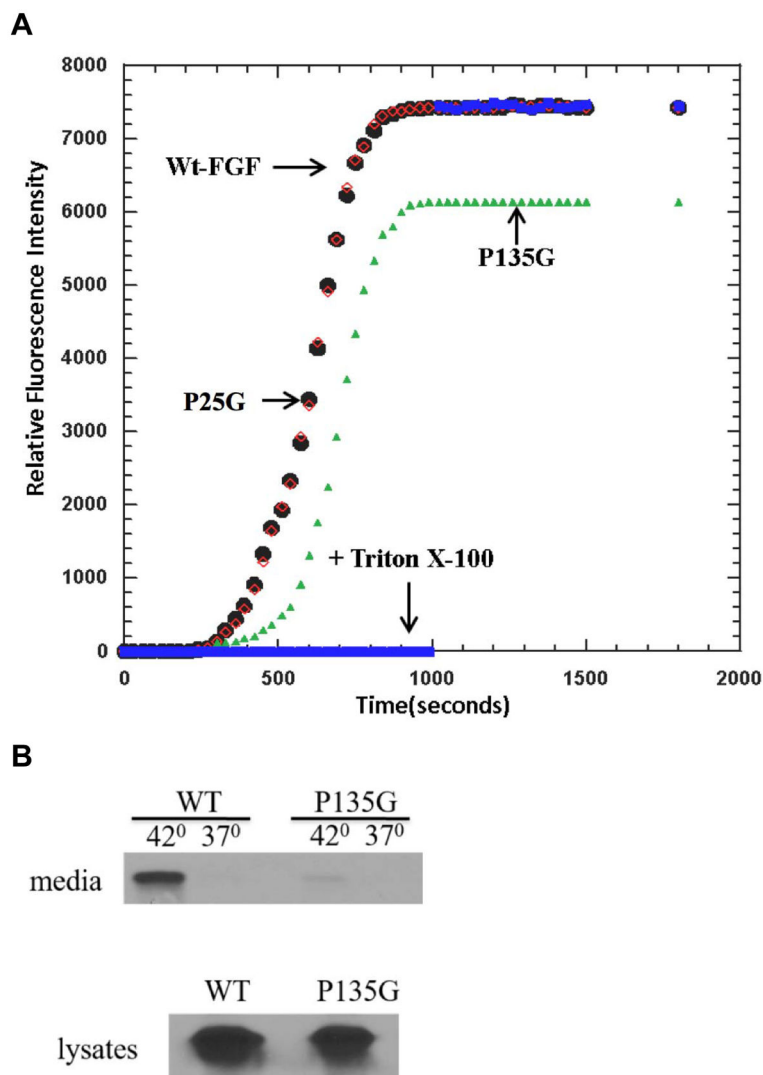


Figure 6. A. Effect of P135G mutation of liposome destabilization by FGF1 and stress-induced release of FGF1

A. P135G (green) FGF1 induces significantly lower release of carboxyfluorescein from PS liposomes than WT (red) and P25G FGF1 (black), which both destabilize liposomes as efficiently as Triton X100 (blue). **B.** NIH 3T3 cells were adenovirally transduced with WT or P135G FGF1 and submitted to 110 min incubation at 37°C or 42°C. FGF1 was isolated from the medium using heparin chromatography, resolved by SDS PAGE and detected using immunoblotting. The release of P135G FGF1 from NIH 3T3 cells is drastically reduced in comparison with WT FGF1.

Table 1

Melting temperatures obtained from DSC experiment with WT FGF1 and proline/glycine mutants.

Protein	T _m [°C]
FGF-1 WT	49.8
FGF-1 WT+SOS	59.3
P25G	46.7
P25G+SOS	57.8
P41G	43.2
P41G+SOS	55.7
P93G	46.0
P93G+SOS	58.9
P135G	45.4
P135G+SOS	57.0
P148G	46.6
P148G+SOS	57.1
P150G	46.6
P150G+SOS	57.1

WT+SOS > P93G+SOS > P25G+SOS > P148G+SOS = P150G+SOS > P135G+SOS > P41G+SOS

WT > P25G > P148G > P93G = P150G > P135G > P41G